Study on the Cracks of NiTiNb/TC4 Lap Joints Welded by Micro Laser Welding

Yuhua Chen, Zilin Zhan, Yuqing Mao, Yangyang Yu and Weiwei Lu

Abstract Dissimilar metal sheets of $Ni_{47}Ti_{44}Nb_9$ (at.%, short for NiTiNb) shape memory alloy and Ti6Al4V (TC4) alloy with the same thickness of 0.2 mm are joined by using micro laser welding technology. The microstructure and crack in the weld are studied by optical microscope (OM) and scanning electron microscope (SEM). The results show that the cracks are easy to generate during the laser lap welding of NiTiNb alloy and TC4 alloy due to plenty of brittle intermetallic compound of Ti_2Ni. However, the welding cracks can significantly reduce or disappear by adding filler metal of Ni foil. No-defect joint is obtained when NiTiNb alloy is located on the upper and 50 μm thick Ni foil is added during the lap welding process. The crack sensitivity can be decreased because of finer grains and elliptic boundaries. The shear load of the joint can reach 162 N.

Keywords NiTiNb/TC4 dissimilar metals · Micro laser welding
Filler metal of Ni · Crack control

1 Introduction

The joining of dissimilar materials is of great significance to the modern industry since single material is unable to meet the needs of a variety of functions for composite structures, so different materials need to be welded to satisfy the multiple uses [1–3]. However, it is easy to produce many cracks during welding dissimilar materials due to the differences in their physical and chemical properties, and the cracks can severely reduce the weld quality such as strength and plasticity.

Y. Chen (✉) · Z. Zhan · Y. Mao (✉) · Y. Yu · W. Lu
School of Aerospace Manufacturing Engineering, Nanchang Hangkong University, Nanchang 330063, China
e-mail: ch.yu.hu@163.com

Y. Mao
e-mail: maoyuqing-8888@163.com

S. Chen et al. (eds.), *Transactions on Intelligent Welding Manufacturing*,
Transactions on Intelligent Welding Manufacturing,
https://doi.org/10.1007/978-981-10-7043-3_5

Therefore, the further application of this welded joint with dissimilar materials is limited [4, 5].

$Ni_{47}Ti_{44}Nb_9$ (at.%, short for NiTiNb) is one of the Ti–Ni shape memory alloys, and it is widely used in aerospace, nuclear industry, offshore oil, household appliances, and daily necessities for its excellent specific strength, corrosion resistance, wear resistance, shape memory effect, and damping properties [6, 7]. Ti6Al4V (TC4) is a kind of titanium alloy that owns both of α and β phases, and it is widely used in biomedical, aerospace, ships and so on for good strength, corrosion resistance, and high temperature resistant performance [8]. The dissimilar material welding of ultra-thin NiTiNb to TC4 could be used for reducing the noise in sound attenuation of aircraft engine components [9]. However, it is easy to produce plenty of brittle intermetallic compound like Ti_2Ni, Ni_3Ti, etc. during the welding process [10, 11]. In addition, Ti alloy can absorb hydrogen from 250 °C, oxygen from 400 °C, and nitrogen from 600 °C [12], which makes it easy to get the brittle joint and generate the welding crack. Therefore, the traditional welding method is difficult to meet the requirements of the TC4 and NiTiNb alloy welding.

Laser welding is one of the important processing methods for the characteristics of high energy density, high precision and so on. Because the power is lower, micro laser welding as one of laser welding technologies commonly used in welding metal sheet, metal wire, and small electronic precision part connection, and it plays an important role in the field of the micro connection field [13, 14]. Li et al. [15, 16] studied the welding of NiTi alloy to stainless steel by adding the metal wire of Ni and Co, and they found that the welding cracks were eliminated. Zoeram and Mousavi [17] found that the transverse cracks were controlled when 1 mm thick NiTi alloy and TC4 alloy were welded by adding filler metal of Cu. Moreover, some high temperature materials such as pure Nb, Ta, and V may also be added to remove the cracks during the welding of TiNi alloy to TC4 alloy [18–20]. However, these materials are rare as well as expensive, so their use is limited.

Therefore in the experiment, micro pulse laser equipment is applied to the lap welding of NiTiNb and TC4 alloy sheets with the same thickness of 0.2 mm, and Ni sheet as a filler metal is used to control the cracks during the welding. The microstructure, crack, and fracture surface of the joint is investigated, and the data can provide the theoretical support for the dissimilar welding of NiTiNb toTC4 alloys.

2 Materials and Methods

In the experiment, 0.3 mm thick NiTiNb hot rolled sheet and 0.2 mm thick TC4 sheet are adopted as a base material. Filler metal of pure Ni foil with a thickness of 50 μm is added in the middle of two alloys during the welding process. Their main chemical components and physical properties are shown in Tables 1 and 2, respectively.

Table 1 Chemical compositions of materials

Element	Mass fraction (%)	
	NiTiNb	TC4
Al	–	5.5
V	–	4.37
Ti	29	90.13
Ni	60	–
Nb	11	–

Table 2 Physical properties of materials

Material	Melting point (°C)	Coefficient of linear expansion × 10^6 ($°C^{-1}$)	Thermal conductivity ($W\ m^{-1}\ °C^{-1}$)	Specific heat capacity ($J\ g^{-1}\ K^{-1}$)
NiTiNb	1250	11.43	9.8	0.461
TC4	1630	9.1	6.8	0.611
Ni	1453	13.3	5.9	0.456

According to ASTM G1-90, NiTiNb alloy sheets are put in a mixed solution (volume ratio, $HF:HNO_3:H_2O$ = 1:3:5) to remove the oxide film before the welding, and then are washed and dried by acetone. The welded NiTiNb alloy sheets must be controlled within 200 ± 10 μm thickness to keep the same thickness as TC4 alloy sheet.

SL-80 type Nd:YAG pulsed laser welding machine is used in the experiment. The laser wavelength is 1.06 μm and the largest laser power is 80 W. The gas protection device is designed in the experiment to prevent the weld from being oxidized. The pure argon gas is filled in the gas box and the gas flow rate is 8 L/min. The process parameters were selected as follows: the laser power is 20 W, the laser spot diameter is 0.3 mm, the pulse width is 6.0 ms, the laser frequency is 5 Hz, and the welding speed is 300 mm/min.

After welding, the microstructure is observed by an optical microscope (OM), and the crack morphologies and fracture surfaces are analyzed by scanning electron microscope (SEM) and energy dispersive spectrometry (EDS).

3 Results and Discussion

3.1 Crack Sensitivity for Different Lap Position

Figure 1 shows the cross section of the joint produced by adding the filler metal of 100 μm thick Ni when NiTiNb alloy is placed on the upper. The macrostructure of the weld presents an onion ring shape which is related to thermal agitation of the laser. In the bottom of the weld, lots of cracks appear near the side of TC4 alloy,

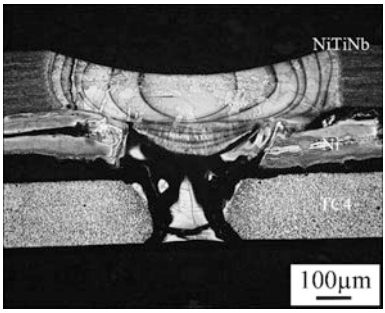

Fig. 1 Cross section of the joint when NiTiNb alloy is placed on the upper and 100 μm thick Ni foil is added

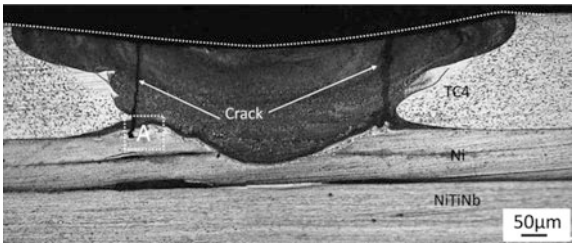

Fig. 2 Cross section of the joint when TC4 alloy is placed on the upper and 100 μm thick Ni foil is added

and the cracking distance is larger. The main reason is that it is easy to generate a large number of brittle intermetallic compounds such as Ti_2Ni and Ni_3Ti in the weld when NiTiNb alloy and TC4 alloy are welded [21]. What is more, the difference of the linear expansion coefficients between NiTiNb alloy and TC4 alloy is large, which makes the weld suffer from large stress concentration. The cracks are easy to generate because of the effect of residual stress during welding. The physical properties of Ni are between those of NiTiNb and TC4 alloys, so it can form metallurgical combination with base material since it can play a buffer action to the welding crack. During welding, this can change the type and number of brittle intermetallic compounds by controlling the melting-mixing ratio of Ni to Ti element according to the Ti–Ni binary phase diagram. Thus, Ni as filler metal can reduce or eliminate the welding cracks during laser welding.

Figure 2 shows the cross section of the joint when TC4 alloy is located on the top during welding. It is clearly seen that two cracks expand upwards from the weld center, the number of cracks significantly decrease and the cracking distance becomes smaller. Figure 3 shows a magnified graph of the crack in the zone A of Fig. 2. It is found that the crack originates from the interface of Ni, fusion zone, and TC4 alloy, and then expands through the grains along the vertical direction. The analysis is that the solidification shrinkage and thermal contraction increase during the cooling process due to the difference in thermal expansion coefficients (the difference of thermal expansion coefficients between TC4 and Ni is bigger than that of TC4 and NiTiNb). The crack produces along the columnar crystal which can urge the inhomogeneous deformation of grains, and add the brittleness and crack sensitivity of the weld.

Fig. 3 Magnified graph in the region A of Fig. 2

3.2 Crack Morphology for Adding Filler Metal

Figure 4 shows the macro cross section when TC4 alloy is placed on the upper and the filler metal of Ni with 50 μm thickness is added during welding. The number of cracks reduces and the cracking distance of the crack is only about 5 μm. Figure 5 shows the local position of the crack. It is seen that the crack originates from the bottom of the weld, different phase structures are layered, and the thickness of compound layers is between 3 and 15 μm in the weld bottom. Lots of shrinkage pores exist near the area of the zone in Fig. 5. The reason is that there is no enough liquid metal supplying from the surrounding of the crack. The EDS result shows that the element proportion of Ti and Ni is 0.83:1 in the zone. However, the element proportion of Ni and Ti in the area is 65.27:28.71, which is close to the ratio of brittle phase of Ti_2Ni. The crack is easy to generate and expand during the process of energy release, and the brittleness of the weld increases.

The cracks can be prevented by reducing the generation of brittle compound [22]. Figure 6a shows the surface morphology of the joint when TC4 alloy is placed on the upper and 50 μm thick Ni filler metal is added during welding. The longitudinal crack occurs on the surface of the joint. However, a no-defect weld is produced when NiTiNb alloy is placed on the upper and 50 μm thick Ni foil is added, as shown in Fig. 6b. Figure 6c shows the cross section of the joint in Fig. 6b when 50 μm thick Ni foil is added. The local cross section of the weld presents chrysanthemum shape which may be related to the thermal agitation of laser during

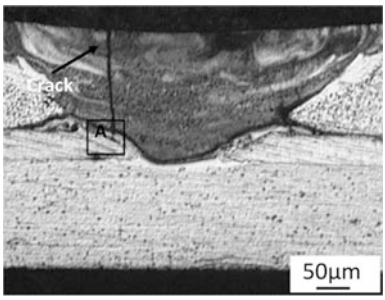

Fig. 4 Cross section of the joint when TC4 alloy is placed on the upper and 50 μm thick Ni foil is added

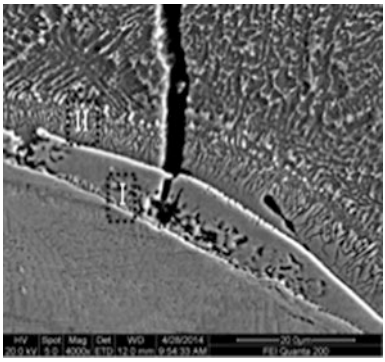

Fig. 5 Magnified graph in the region A of Fig. 4

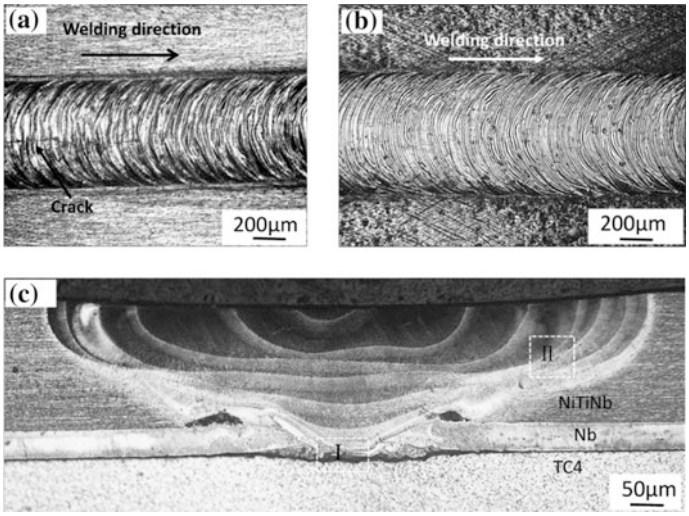

Fig. 6 Surface morphology when TC4 alloy: **a** or NiTiNb alloy; **b** is placed on the upper and cross-sectional morphology; **c** of the joint in Fig. 6b

the welding process. Also, the width of the upper molten pool is wider than that in the bottom. However, it is similar to the "bowl" shape for the whole weld due to heat transfer. High temperature is produced by laser focusing which can cause the loss of alloy elements, so the top shape of the weld is concave. The closed metallurgical combination is formed, and the defects such as blowholes and cracks are not found in the weld. Different organizations can be seen in the weld, which suggests that the macro segregation is coming.

3.3 Distribution of Element

Figure 7 shows an enlarged map of the area I in Fig. 6c. The layered microstructure is obvious in the bottom of the melted pool that presents different phase structures. A transition layer with a width of 10 μm is adjacent to the base material. Table 3 shows the result of EDS analysis in the area in Fig. 6c. The content of Ni in the area of Point C is the highest, and then reduces with the increase of the distance from Point C. However, the content of Ti element becomes higher with the increase of the distance from Point C, and it is close to that of TC4 at Point A and that of TiNiNb at Point E, respectively. The content of Nb gradually decreases from Point E to Point A. The reason is that Point C is in the area of Ni sheet. Al and V elements gradually reduce in the fusion zone along the vertical direction to the weld surface. The result in Table 4 shows that the black area lacks V element while the white area contains V element. The content of Al near weld surface reduces and it is about 0.14% in the area of in Fig. 6c. Point B mainly contains Ni element and Ti element; the ratio of Ni to Ti is about 31.26:60.21. It is proved that this area is Ti_2Ni phase according to the studies of Song et al. [23] and Chen et al. [24] and Ti–Ni binary phase diagram. The existence of brittle Ti_2Ni phase can increase the crack sensitivity and reduce the toughness of the weld.

Figure 8 shows a magnified map of the area II in Fig. 6c. In the weld center, the heat dissipation is slower than that far from this area, which can form the dendrite in bar shape. However, the supercooling degree of the right area far from the weld center is larger than that of the weld center because of faster heat dissipation, so like

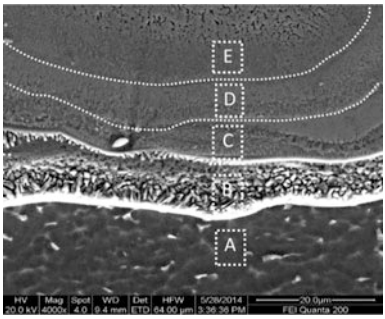

Fig. 7 Microstructure in the bottom of the weld

Table 3 EDS analysis in the bottom of the weld when NiTiNb alloy is placed on the upper and 50 μm thick Ni foil is added

Point	Element content (at.%)				
	Ni	Ti	Nb	V	Al
A	–	88.89	–	3.81	7.30
B	31.26	60.21	0.48	4.57	3.48
C	59.58	33.68	2.57	1.54	2.63
D	55.04	38.84	6.12	–	–
E	40.89	47.30	11.25	–	0.56

Table 4 EDS analysis when NiTiNb alloy is placed on the upper

Point	Element content (at.%)				
	Ni	Ti	Nb	V	Al
F	47.45	46.56	5.85	–	0.14
G	43.03	46.59	9.57	0.67	0.14

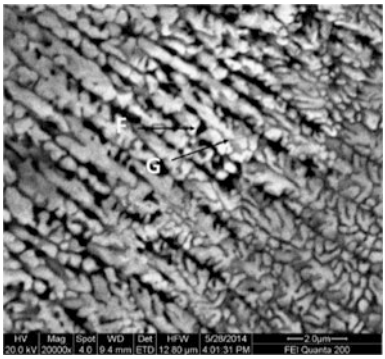

Fig. 8 SEM image in the area of Fig. 6c

the parent metal on the right, the grain size is finer. Little V element is found at Point G from Table 4, but Point F lacks V element. The content of Nb element at Point F is higher than that at Point G. The content of Nb element in the white area is higher than that in the black area. In general, the black areas are low-melting eutectic zones, and the gap can be filled by crystal grains, so the crystallization crack is prevented [25]. The compositions in these regions are uniformly distributed and the small grain and elliptic boundaries are formed in the weld. These conditions are very helpful for avoiding the stress concentration. Therefore, the cracks in the weld obviously decrease even disappear.

3.4 Fracture Surface

When NiTiNb alloy is placed on the upper and 50 μm thick filler metal of Ni is added during welding, the tensile test of the joint is carried out and the fracture surface is analyzed. Figure 9 shows the load-displacement curve of the tensile sample. It is seen that the shear load is about 162 N. Figure 10 shows the SEM image of the fracture surface of the tensile sample. The macro fracture is flat and the cleavage stage is found in local region of fracture surface. Also, few micro-cracks are observed. The main reason is that large stress concentration occurs due to brittle compounds generated by composition segregation. During the testing process, the cracks rapidly expand to the surrounding when the load is greater than the yield strength of the weld and the brittle fracture occurs.

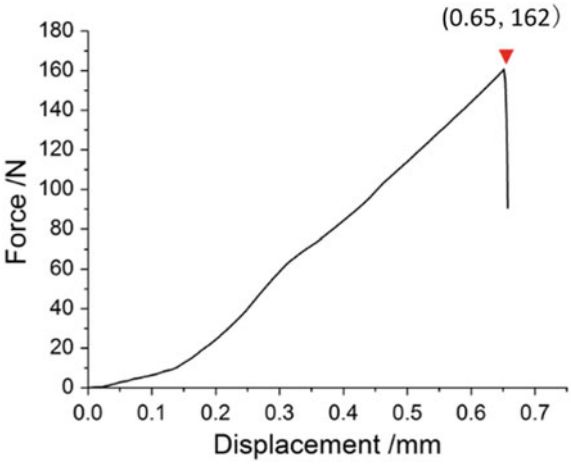

Fig. 9 Load-displacement curve when NiTiNb alloy is placed on the upper and 50 μm thick Ni foil is added

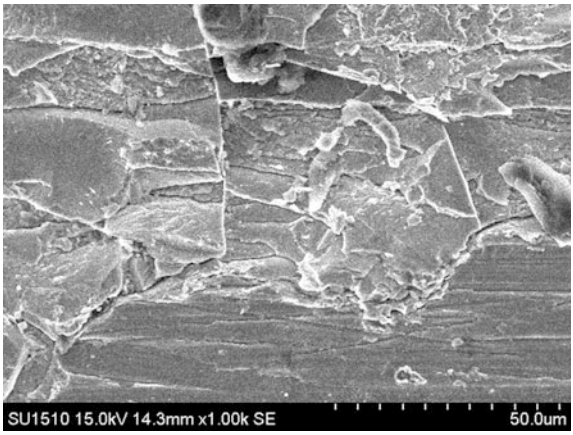

Fig. 10 SEM image of fracture surface

4 Conclusion

(1) Lots of cracks are generated when NiTiNb alloy and TC4 alloy are joined by laser welding due to brittle intermetallic compounds. The decrease and elimination of the cracks in the joint can be controlled by adding filler metal of Ni with different thicknesses and a no-defect joint can be obtained.

(2) The crack sensitivity of the joint increases due to the formation of Ti_2Ni brittle compounds. The finer grains and elliptic boundaries are formed when filler metal of Ni is added during the welding process, which can prevent the crack from the formation and reduce the crack sensitivity.

(3) When NiTiNb alloy is placed on the upper and 50 μm thick filler metal of Ni is added, no crack is found on the surface and the cross section of the weld. The shear load of the joint can reach 162 N and the fracture mechanism presents a brittle fracture.

Acknowledgements The research is supported by the National Natural Science Foundation of China (51565040), the Aviation Science Funds (2014ZE56016), the Jiangxi Science and Technology Plan Projects (20151BBE50034), and the State Key Laboratory of Advanced Welding and Connection Open Topics (AWJ-M15-03).

References

1. Sonato M, Piccolroaz A, Miszuris W et al (2015) General transmission conditions for thin elasto-plastic pressure-dependent interphase between dissimilar materials. Int J Solids Struct 64:9–21
2. Volkov SS, Kholopov YV (1998) Technology and equipment for ultrasonic welding of polymer based composite structures. Russ Ultrason 28(4):145–155
3. Wei YN, Li JL, Xiong JT et al (2015) Research status on friction stir welding of aluminum/steel dissimilar metals. J Netshape Form Eng 7(5):34–40
4. Miranda RM, Assuncao E, Silva RJC et al (2015) Fiber laser welding of NiTi to Ti-6Al-4V. Int J Adv Manuf Technol 81(9):1533–1538
5. Zoeram AS, Mousavi SAAA (2014) Laser welding of Ti-6Al-4V to Nitinol. Mater Des 61:185–190
6. Zhou JB, Wang KL, Chen Q et al (2014) Calculation of the pull-out force of $Ni_{47}Ti_{44}Nb_9$ shape memory ally pipe coupling. Appl Mech Mater 697:360–364
7. Piotrowski B, Zineb TB, Ebehardt A et al (2011) Experimental analysis of $Ni_{47}Ti_{44}Nb_9$ shape memory alloy behavior for tightening application numerical design. Proc Int Symp Steel Struct 258:331–338
8. Li GR, Li YM, Wang FF et al (2015) Microstructure and performance of solid TC4 titanium alloy subjected to the high pulsed magnetic field treatment. J Alloy Compd 644:750–756
9. Mabe J (2008) Variable area jet nozzle for noise reduction using shape memory alloy actuators. J Acoust Soc Am 123:3871–3876
10. Fokin VN, Fokina EE, Korobov II et al (2014) Hydriding of intermetallic compound Ti_2Ni. Russ J Inorg Chem 59:1073–1076
11. Mullner P (1999) Shape memory alloys. Mater Sci Eng 268:246–247
12. Montanari R, Costanza G, Tata ME et al (2008) Lattice expansion of Ti-6Al-4V by nitrogen and oxygen absorption. Mater Charact 59(3):334–337
13. Zhang C, Sun X (2013) Susceptibility to stress corrosion of laser-welded composite arch wire in acid artificial saliva. Adv Mater Sci Eng 46(13):171–177
14. Shelyagin VD, Orishich AM, Khaskin V et al (2014) Technological peculiarities of laser, microplasma and hybrid laser-microplasma welding of aluminium alloys. Paton Weld J 5:33–39
15. Li HM, Sun DQ, Dong P et al (2012) Analysis and prevention of cracks in laser-welded joint of TiNi shape memory alloy and stainless steel. Trans China Weld Inst 33(12):41–44
16. Li HM, Sun DQ, Dong P et al (2011) Study on Laser welding of dissimilar materials between TiNi shape memory alloy/stainless steel. J Mater Eng 1(10):47–51
17. Zoeram AS, Mousavi SAAA (2014) Effect of interlayer thickness on microstructure and mechanical properties of as welded Ti6Al4V/Cu/NiTi joints. Mater Lett 133:5–8

18. Oliveira JP, Panton B, Zeng Z et al (2016) Laser joining of NiTi to Ti6Al4V using a niobium interlayer. Acta Mater 105:9–15
19. Haas T, Schuessler A (1999) Welding and joining of TiNi shape memory alloys: engineering aspects and medical applications. In: Proceedings of the 1st European conference on shape memory and superelastic technologies, SMST, Paris, pp 103–114
20. Lu L (2012) Research on electron beam welding of TC4 titanium alloy and 304 stainless steel. Dissertation, Nanjing University of Technology, China
21. Oliveira JP, Panton B, Zeng Z et al (2016) Laser joining of NiTi to Ti-6Al-4V using a niobium interlayer. Acta Mater 105:9–15
22. Hu P, Zhang H, Zhang XZ et al (2014) Application of a corner chamfer to steel billets to reduce risk of internal cracking during casting with soft reduction. ISIJ Int 54(10):2283–2287
23. Song P, Zhu Y, Guo W et al (2013) Mechanism of crack formation in the laser welded joint between NiTi shape memory alloy and TC4. Rare Metal Mater Eng 4:6–9
24. Chen YH, Mao YQ, Lu WW et al (2017) Investigation of welding crack in micro laser welded NiTiNb shape memory alloy and Ti6Al4V alloy dissimilar metals joints. Opt Laser Technol 91:197–202
25. Min P, Shuichi M, Kazuhiro O et al (1992) Effects of Nb addition on the microstructure of Ti-Ni alloys. Mater Trans, JIM 33(4):337–345